Chapter 8

ACTIVATION MEASUREMENTS FOR THERMAL NEUTRONS

Part G. Natural ^{36}Cl Production in Mineral Samples

Eckehart Nolte, Thomas Huber, Werner Rühm, Kazuo Kato, Vitali Lazarev, Ludolf Schultz

Introduction

After the publication of DS86 (Roesch 1987), an increasing number of measurements were made of thermal neutron activation products such as ^{36}Cl, ^{60}Co and ^{152}Eu in Hiroshima at ground ranges beyond 1,000 m. Our investigations of the natural *in situ* production of radionuclides by the nucleonic and the muonic component of cosmic rays and by neutrons originating from uranium (U) and thorium (Th) decay had indicated already in the past that as much as several millions of atoms per gram of long-lived radionuclides such as ^{26}Al, ^{36}Cl and ^{53}Mn are being produced in saturation in the lithosphere (Dockhorn et al. 1991; Heisinger et al. 1997, 2002a,b; Heisinger and Nolte 2000; Hagner et al. 2000). If one bears in mind that 10^5 atoms of ^{36}Cl would correspond to an isotopic ratio of ^{36}Cl/Cl = 6×10^{-14} in a matrix containing 100 ppm of stable chlorine, which is a typical value for granite, and that a similar ratio is induced by neutrons from the Hiroshima bomb at a ground range of about 1,400 m, it becomes evident that a detailed investigation of the natural *in situ* production of the long-lived ^{36}Cl in the lithosphere is indispensable, if measurements of thermal neutron activation in distant samples at both Hiroshima and Nagasaki are to be interpreted correctly. It should be noted at this point, however, that natural *in situ* production of short-lived radionuclides such as ^{60}Co and ^{152}Eu is not considered to play any important role in distant samples at Hiroshima and Nagasaki, because of the short accumulation time of these radionuclides due to their short half-lives.

For mineral samples from Hiroshima, natural *in situ* production of ^{36}Cl by the nucleonic component of cosmic radiation, by stopped negative muons and by fast muons, and by neutron capture reactions where the neutrons originate from the above reactions and from the U and Th decays was treated theoretically. In order to calculate *in situ* production due to cosmic radiation, several factors must be known. Among those are the elemental composition of the investigated

material, the depth at which it was found in the lithosphere, and the local erosion rate. Taking these factors into account, we present here a comparison between ^{36}Cl/Cl ratios measured by means of accelerator mass spectrometry (AMS) on granite samples not exposed to A-bomb neutrons, and those calculated for non-exposed samples.

Materials and Methods

Calculation of Natural In Situ Production of ^{36}Cl

In the granite of the lithosphere, ^{36}Cl is produced by four reaction mechanisms (Heisinger et al. 2002a,b): spallation and nuclear reactions of the nucleonic component of the cosmic rays with potassium and calcium nuclei; particle emission after μ^- capture in potassium and calcium nuclei; reactions of fast muon induced hadronic and electromagnetic showers with potassium and calcium nuclei; and neutron capture reactions on ^{35}Cl where the neutrons originate from spallation reactions, μ^- capture, fast muon induced reactions, and U and Th decays (Feige et al. 1968).

The production of radionuclides in the lithosphere depends on the thickness of the over-lying rock layer that acts as a shield against cosmic rays. Therefore, the lithospheric depth of the investigated sample is an important parameter that governs the production due to cosmic radiation. Local erosion rates have to be known, since they determine the lithospheric depth of a sample averaged over the lifetime of the radionuclide or the mineral. The concentrations of potassium, calcium, thorium and uranium have to be known as well as the chemical composition of the sample, in order to be able to calculate the fraction of neutrons that are captured by ^{35}Cl and produce ^{36}Cl.

Calculated depth profiles that describe the production of radionuclides in the lithosphere by the nucleonic component, by stopped negative muons and by fast muons can be taken from Heisinger et al. (2002a,b). For simplicity, the depth profiles given there can be approximated by exponential functions with attenuation lengths of Λ_h = 150 g/cm^2 for the nucleonic component, $\Lambda_{\mu\_}$ = 1,510 g/cm^2 for stopped negative muons, and Λ_{μ_f} = 4,320 g/cm^2 for fast muons, respectively.

The calculated production of ^{36}Cl by thermal neutrons is based on the assumption that all neutrons originating from the interaction of cosmic radiation with the lithosphere or from U and Th decay are thermalized without losses, and that only thermal neutron capture reactions contribute. To account for absorption of epithermal neutrons or for reactions other than thermal neutron captures, correction factors f_{norm} would have to be introduced into the calculations. These correction factors are expected to be close to unity and are not considered in our calculations.

Production of ^{36}Cl due to the Nucleonic Component of the Cosmic Rays

If the data from Heisinger et al. (2002a,b) are corrected for the geomagnetic latitude at Hiroshima (Lal 1991), the production rate $P_h(0)$ of ^{36}Cl due to the nucleonic component of the cosmic rays at sea level is given by

$$P_h(0) = \left(h(K)\cdot 140 + h(Ca)\cdot 37.2 + 1915\cdot f(^{36}Cl)\right) g^{-1}a^{-1} \quad (1)$$

The first two terms describe the production rates by spallation and by nuclear reactions on K and

Ca in a matrix with mass abundances h(K) and h(Ca), respectively. The third term describes the production by thermalized neutrons by the nucleonic component. Approximately, the fraction f(^{36}Cl) of neutrons producing the radionuclide ^{36}Cl is given by

$$f(^{36}Cl) = \frac{a(^{35}Cl) \cdot \sigma(^{35}Cl(n_{th},\gamma)^{36}Cl)}{\sum a(Z) \cdot \sigma_{th}(Z)} \tag{2}$$

with a particle abundance $a(Z)$ and thermal neutron absorption cross section $\sigma_{th}(Z)$ for the element Z, and a particle abundance $a(^{35}Cl)$ and thermal neutron absorption cross section $\sigma(^{35}Cl(n_{th},\gamma)^{36}Cl)$ for ^{35}Cl.

Production of ^{36}Cl due to Capture of Negative Muons

The production rate due to capture of negative muons is given by

$$\begin{aligned} &P_{\mu^-}(0) = \\ &\left(f_C(K) \cdot f_D(K) \cdot f^*(K \rightarrow {}^{36}Cl) + f_C(Ca) \cdot f_D(Ca) \cdot f^*(Ca \rightarrow {}^{36}Cl) + n_{\mu^-}(n) \cdot f(^{36}Cl) \cdot 190\right) g^{-1} a^{-1} = \\ &\left(f_C(K) \cdot 5.33 + f_C(Ca) \cdot 7.26 + n_{\mu^-}(n) \cdot f(^{36}Cl) \cdot 190\right) g^{-1} a^{-1} \end{aligned} \tag{3}$$

where

$$f_C(Z) = \frac{a(Z) \cdot P(Z)}{\sum a(Z) \cdot P(Z)} \tag{4}$$

is the chemical compound factor with the average atomic capture probabilities $P(Z)$ relative to oxygen given by von Egidy and Hartmann (1982), f_D is the probability that a stopped μ^- does not decay before nuclear capture (Suzuki et al. 1987), f^* is the probability that ^{36}Cl is produced after nuclear μ^- capture (Heisinger et al. 2002b), and

$$n_{\mu^-}(n) = \sum f_C(Z) \cdot f_D(Z) \cdot f_n(Z) \tag{5}$$

is the mean number of produced neutrons per μ^- capture in the considered mineral. The mean number $f_n(Z)$ of neutrons emitted from the element Z is taken from Singer (1974).

The first two terms in Equation (3) describe production of ^{36}Cl by μ^- capture in K and Ca, respectively. The third term describes production by neutron capture reactions, where the neutrons are emitted after nuclear capture.

Production of ^{36}Cl due to Fast Muons

The production rate due to reactions with fast muon induced hadronic and electromagnetic showers is given by

$$P_{\mu_f}(0) = \left(h(K) \cdot 3.49 + h(Ca) \cdot 0.739 + 12.2 \cdot f(^{36}Cl)\right) g^{-1} a^{-1} \tag{6}$$

The first two terms describe production of ^{36}Cl by fast muon induced shower reactions on K and Ca, respectively. The third term describes production by fast muon produced neutrons.

Production of ^{36}Cl due to Neutrons from U and Th Decay

The production rate $P_{U,Th}$ of ^{36}Cl by neutrons originating from spontaneous fission of ^{238}U and from (α,n) reactions with α particles following decays of ^{232}Th, ^{235}U and ^{238}U is taken from Feige et al. (1968).

Concentration of ^{36}Cl due to Natural In Situ Production

With the simplified exponential depth dependences for muon induced reactions mentioned above, the total production rate of ^{36}Cl, $P(h)$, as function of depth h in the lithosphere is given by

$$P(h) = P_h(0) \cdot e^{-\frac{h}{1.5hg/cm^{-2}}} + P_{\mu^-}(0) \cdot e^{-\frac{h}{15.1hg/cm^{-2}}} + P_{\mu_f}(0) \cdot e^{-\frac{h}{43.2hg/cm^{-2}}} + P_{U,Th} \tag{7}$$

where unit hg/cm^2 corresponds to meter water equivalent (mwe) and translates to depth in meter, if divided by the rock density.

The number of radionuclides per gram, N(h), at depth h below a surface, which is eroding with a rate ε and over a time period t is then calculated to be:

$$N(h) = \int_0^t dt' \cdot P(h + \varepsilon \cdot t') \cdot e^{-\frac{t'}{\tau}} \tag{8}$$

with τ being the lifetime of the radionuclide of interest.

In granite or concrete, the natural ^{36}Cl concentration per gram thus depends on the chemical composition of the investigated sample, on the local erosion rate at the quarry and the depth where the granite or the constituents of the concrete were taken.

In the calculations shown in Figures 1 to 8, the depth dependent functions (Heisinger et al. 2002a,b) were used rather than the exponential approximations given above.

New Granite Samples Not Exposed to A-Bomb Neutrons

To assess the natural ^{36}Cl level in the investigated granite samples experimentally, we looked for new granite samples from quarries near Hiroshima. Samples of four different local granite types, Aji, Giin, Iyo and Odachi, were chosen. Information on the depths from which these granite samples came was obtained by means of detailed interviews of miners of granite and owners of granite quarries. These interviews indicated that the sample from the Aji quarry on Shikoku Island (Aji-cho, Kagawa Pref.) was taken from 10-30 m depth. The Iyo-type sample from Oshima Island (Miyakubo-cho, Ehime Pref.) was supposedly taken from 5-60 m depth. From Kurahashi Island (Kurahashi-cho, Hiroshima Pref.), two types of granite were obtained. The Giin-type sample was supposedly taken from 10-30 m depth, whereas the Odachi-type sample was supposedly taken from 7-100 m depth (Oda 2001; Nakano 2001; Tanimura 2001).

The chemical composition of these four samples was determined by the XRAL Company, and the ^{36}Cl/Cl ratios measured, by means of AMS at Munich (Kubik et al. 1983, 1984; Haberstock et al. 1986). The physical and chemical processing of the granite samples, and the AMS measurements were performed in the same way as described in Chapter 8, Part E of this report.

Old Granite Samples Exposed to A-Bomb Neutrons

A couple of distant granite samples exposed to A-bomb neutrons were also investigated. Detailed interviews of manufacturers of granite and of owners of granite quarries indicated that, before the war, granite was taken most probably from a depth between 5 and 15 m from the surface of the Earth (Oda 2001; Nakano 2001; Tanimura 2001). The chemical composition of these samples was also determined by XRAL Company.

Results and Discussion

Determination of Elemental Composition and of Local Erosion Rates by Means of the ^{40}K - ^{40}Ar Method

The elemental composition of the investigated samples from the various quarries was determined from the measurements by the XRAL Company (see Tables 1 and 2), and the erosion rate at the site of the quarries was determined from the argon (Ar) age of the sample.

In previous studies of a sample from the Aji quarry, the potassium concentration was determined to be 2.5% (Rühm 1993). After noble gas extraction and cleaning, 1.44×10^{-5} cm^3 STP/cm^3 (STP: Standard Temperature and Pressure) of ^{40}Ar was measured in this sample by conventional mass spectrometry, and the ^{40}Ar/^{36}Ar ratio was determined to be 1,090 ± 20. From the deduced concentration of ^{40}K and from the excess ^{40}Ar by decay, an Ar age of 108 million years was calculated. This agrees well with an age of 83.5 million years estimated for the Aji-stone (Yuhara 1999). With an Ar retention temperature of 350°C corresponding to a depth of about 11 km in the lithosphere, an erosion rate of $\varepsilon = 100$ $\mu m/a$ was obtained.

From the Iyo-type granite (actually this sample was part of a gravestone from the Shinkoji graveyard, 818 m from the hypocenter (Chapter 8, Part E) 40.7 g of biotite was separated (Tolstikhin 2003) containing 2.6 g of K. After noble gas extraction and cleaning, the ^{40}Ar excess due to decay of ^{40}K was obtained to be $(849 \pm 50)\cdot 10^{-6}$ cm^3 STP (Tolstikhin 2003). From the ratio of radiogenic ^{40}Ar to ^{40}K, an Ar age of 86 million years was deduced and an erosion rate of $\varepsilon =$ 128 $\mu m/a$ was calculated.

Both values are in full agreement with expected typical erosion rates for this region of about $\varepsilon = (80 – 330)$ $\mu m/a$ (Fujiwara et al. 1992).

Calculated ^{36}Cl Depth Profiles in Granite

For the quarry granite samples and for several of the exposed large-distance granite samples that had been exposed to A-bomb neutrons (Chapter 8, Part E), the natural *in situ* production of ^{36}Cl was calculated based on their elemental compositions (Tables 1 and 2) and on erosion rates of $\varepsilon = 50$, 100 and 200 $\mu m/a$, respectively. Figures 1 through 4 show the resulting ^{36}Cl concentrations $N(h)$ per gram granite as function of depth h in $hg/cm^{-2} = mwe$ (meter water equivalent), for the granite samples from the Aji, Iyo, Giin and Odachi quarries.

Figures 5 through 8 show the ^{36}Cl concentrations $N(h)$ per gram granite as function of depth h in $hg/cm^{-2} = mwe$ (meter water equivalent), again calculated for erosion rates of $\varepsilon = 50$, 100 and 200 $\mu m/a$, for large-distant granite samples exposed to A-bomb neutrons (see Chapter 8, Part E: Ganjyoji 1 and 2, Hosenji 1, 2 and 3, Tokueiji, Jyunkyoji, ditch cover and facade of the E-building, and Postal Savings Office). The corresponding $^{36}Cl/Cl = 10^{-13}$ ratio is drawn as a

horizontal line.

As described by equations (7) and (8), the depth profiles shown in Figures 1 through 8 decrease with increasing depth from the surface. A high nominal erosion rate of $\varepsilon = 200\ \mu m/a$ means that a sample found today in a certain depth was located in greater depth in the past, shielded more effectively against cosmic rays and, therefore, shows lower ^{36}Cl concentrations compared to a sample from an area with lower nominal erosion rates of $\varepsilon = 100\ \mu m/a$ and $\varepsilon = 50\ \mu m/a$.

For minerals with high U/Th contents, the ^{36}Cl concentrations have a weak dependence on depth. In contrast, for Aji-type granite with its low uranium and thorium content of 0.8 ppm and 6.6 ppm, respectively, the ^{36}Cl profile is comparably steep. Production due to neutrons from U and Th decays become important at about 100 mwe (about 37 m; see Figure 1). At great depths, the ^{36}Cl concentration levels off at about 3×10^4 ^{36}Cl atoms/g and reaches, with a stable chlorine content of 100 ppm, a $^{36}Cl/Cl$ ratio of about 2×10^{-14}.

Table 1. Elemental composition determined by XRAL Company for four types of local Hiroshima granite

Elements	XRAL method code	units	Detection limit	Aji	Giin A[a]	Giin B[a]	Iyo A[a]	Iyo B[a]	Odachi
SiO_2	XRF100	%	0.01	71.4	75.2	74.8	72.7	72.9	74.5
Al_2O_3	XRF100	%	0.01	15.1	13	13.4	14.2	14.1	13.4
CaO	XRF100	%	0.01	3.03	1.39	1.37	2.31	2.26	1.87
MgO	XRF100	%	0.01	0.58	0.24	0.23	0.34	0.35	0.3
Na_2O	XRF100	%	0.01	3.93	3.4	3.4	3.86	3.67	3.57
K_2O	XRF100	%	0.01	2.31	4.4	4.62	3.23	3.25	3.77
Fe_2O_3	XRF100	%	0.01	2.47	1.93	1.97	2.73	2.72	2.38
MnO	XRF100	%	0.01	0.05	0.04	0.04	0.06	0.06	0.05
TiO_2	XRF100	%	0.001	0.295	0.147	0.15	0.204	0.222	0.205
P_2O_5	XRF100	%	0.01	0.07	0.02	0.02	0.05	0.05	0.03
Cr_2O_3	XRF100	%	0.01	0.02	0.01	0.02	0.01	0.02	0.01
LOI[b]		%		0.6	0.4	0.4	0.4	0.5	0.25
Sum		%		99.9	100.2	100	100.1	100	100.3
Be	ICP80	ppm	0.5	1.4	2.7	2.6	2	2	2.8
Na	ICP80	%	0.01	2.72	2.47	2.45	2.69	2.77	2.54
Mg	ICP80	%	0.01	0.31	0.1	0.11	0.16	0.17	0.15
Al	ICP80	%	0.01	7.87	6.22	7.44	6.34	6.79	6.94
P	ICP80	%	0.01	0.03	0.01	0.01	0.02	0.02	0.02
K	ICP80	%	0.01	1.89	3.69	3.95	2.73	2.93	3.18
Ca	ICP80	%	0.01	1.73	0.84	0.82	1.34	1.33	1.12
Sc	ICP80	ppm	0.5	3	3.9	4.2	4.3	4.5	4.5
Ti	ICP80	%	0.01	0.16	0.09	0.09	0.12	0.12	0.12
V	ICP80	ppm	2	11	7	7	6	6	9
Cr	ICP80	ppm	1	38	40	44	35	52	34
Mn	ICP80	ppm	2	313	311	312	432	447	370
Fe	ICP80	%	0.01	1.49	1.23	1.27	1.65	1.71	1.51

Table 1. Continued

Elements	XRAL method code	units	Detection limit	Aji	Giin A[a]	Giin B[a]	Iyo A[a]	Iyo B[a]	Odachi
Co	ICP80	ppm	1	5	3	3	4	4	3
Ni	ICP80	ppm	1	4	7	4	5	4	4
Cu	ICP80	ppm	0.5	7.9	4.9	5.3	4	4.3	5.3
Zn	ICP80	ppm	0.5	53.2	54.4	53.5	59.1	61.4	60.5
As	ICP80	ppm	3	11	<3	8	<3	<3	8
Sr	ICP80	ppm	0.5	356	77.4	78.4	198	203	105
Y	ICP80	ppm	0.5	5.8	25	24	16.1	16	28.4
Zr	ICP80	ppm	0.5	3.8	22.3	24	11.1	11	20.4
Mo	ICP80	ppm	1	2	2	<1	2	2	<1
Ag	ICP80	ppm	0.2	0.4	0.4	0.4	0.4	<0.2	<0.2
Cd	ICP80	ppm	1	<1	<1	<1	<1	<1	<1
Sn	ICP80	ppm	10	<10	<10	11	<10	<10	<10
Sb	ICP80	ppm	5	<5	<5	<5	<5	<5	<5
Ba	ICP80	ppm	1	530	358	374	516	569	386
La	ICP80	ppm	0.5	21.2	15.4	14.4	17.2	18.3	23
W	ICP80	ppm	10	<10	<10	<10	<10	<10	<10
Pb	ICP80	ppm	2	11	20	17	14	17	21
Bi	ICP80	ppm	5	<5	<5	<5	<5	<5	<5
Li	ICP80	ppm	1	32	84	83	49	52	77
B	ES_4	ppm	10	<10	<10	<10	<10	<10	<10
Y	MS90	ppm	1	13	44	42	25	25	44
La	MS90	ppm	0.1	34.9	23.1	20.1	24.1	27.4	30.8
Ce	MS90	ppm	0.1	64.7	50.2	44.1	48.1	54.5	65.8
Nd	MS90	ppm	0.1	24.1	22.6	21.5	22.6	24.6	29
Sm	MS90	ppm	0.1	4.3	6.1	5.9	4.9	5.2	7
Eu	MS90	ppm	0.05	0.76	0.41	0.53	0.78	0.82	0.59
Gd	MS90	ppm	0.1	3.9	7.2	6	5	5	6.9
Tb	MS90	ppm	0.1	0.5	1.2	1.1	0.8	0.7	1.1
Dy	MS90	ppm	0.1	2.4	7.8	6.7	4.6	4.7	7.1
Ho	MS90	ppm	0.05	0.4	1.39	1.4	0.8	0.85	1.42
Er	MS90	ppm	0.1	1.2	4.7	4.4	2.5	2.6	4.7
Tm	MS90	ppm	0.1	0.2	0.7	0.7	0.4	0.4	0.7
Yb	MS90	ppm	0.1	1.1	4.6	4	2.6	2.6	5
Lu	MS90	ppm	0.05	0.11	0.65	0.65	0.38	0.37	0.64
Th	MS90	ppm	0.1	6.6	21.5	18.1	9.2	11.1	20.9
U	MS90	ppm	0.1	0.8	4	4.2	2.2	2.1	5.5
Pr	MS90	ppm	0.1	7.5	6.5	5.6	5.9	6.8	8.2
Cl	CHM113	ppm	50	98	102	102	88	98	87

[a]Two aliquots from Giin-type (Giin A, B) and Iyo-type (Iyo A, B) granite were measured to test the reproducibility of the analyses.

[b]Loss of ignition.

Table 2. Elemental composition determined by XRAL Company for distant granite samples from Hiroshima exposed to A-bomb neutrons (see Chapter 8, Part E)

Element	XRAL Method Code	Unit	Detection limit	PSO[b]	EP1[c]	EB1 G[d]	EB1 B[e]	Jyun[f]	Tok[g]	Gan1[h]	Gan2[h]	Hos1[i]	Hos2[i]	Hos3[i]
SiO_2	XRF100	%	0.01	73.5	74.2	76.1	69.5	75.8	74.8	74.7	74.5	74	72.8	73.4
Al_2O_3	XRF100	%	0.01	13.4	13.6	12.9	8.84	13	13	13.1	13.1	14	13.9	13.8
CaO	XRF100	%	0.01	1.48	1.33	1.09	9.02	1.38	1.53	1.76	1.61	1.43	2.08	2.11
MgO	XRF100	%	0.01	0.4	0.16	0.18	0.82	0.27	0.42	0.47	0.46	0.28	0.56	0.28
Na_2O	XRF100	%	0.01	3.43	3.83	3.35	1.77	3.55	3.17	3.23	3.23	3.7	3.37	3.64
K_2O	XRF100	%	0.01	4.3	4.24	4.56	2.13	3.84	4.41	3.93	4.2	4.13	3.88	3.35
Fe_2O_3	XRF100	%	0.01	1.89	1.96	1.29	2.5	1.93	2.08	2.24	2.3	1.84	2.69	2.74
MnO	XRF100	%	0.01	0.04	0.05	0.03	0.06	0.04	0.05	0.05	0.06	0.04	0.06	0.06
TiO_2	XRF100	%	0.001	0.173	0.125	0.085	0.26	0.156	0.19	0.214	0.213	0.152	0.264	0.185
P_2O_5	XRF100	%	0.01	0.02	<0.01	<0.01	0.05	0.02	0.03	0.03	0.04	0.02	0.05	0.04
Cr_2O_3	XRF100	%	0.01	0.02	0.01	0.02	<0.01	0.02	0.02	0.02	0.01	0.01	0.02	0.02
LOI[a]		%		0.55	0.55	0.4	4.1	0.4	0.3	0.2	0.35	0.4	0.4	0.4
Sum		%		99.2	100.1	100	99.1	100.3	100	99.9	100.1	100	100.1	100
Be	ICP80	ppm	0.5	5.6	2.1	1.8	0.9	2.9	1.9	2.2	1.7	3.6	2	1.8
Na	ICP80	%	0.01	2.47	2.6	2.4	1.21	2.39	2.16	2.36	2.26	2.63	2.54	2.57
Mg	ICP80	%	0.01	0.13	0.06	0.07	0.44	0.12	0.2	0.26	0.23	0.13	0.31	0.13
Al	ICP80	%	0.01	6.48	6.84	6.09	3.97	5.76	7.4	7.12	6.58	6.41	7.6	6.34
P	ICP80	%	0.01	0.01	<0.01	<0.01	0.02	0.01	0.02	0.02	0.02	0.01	0.03	0.02
K	ICP80	%	0.01	3.66	3.42	3.86	1.64	3.04	3.57	3.41	3.43	3.6	3.42	2.83
Ca	ICP80	%	0.01	0.82	0.77	0.66	5.27	0.78	0.91	1.1	0.93	0.84	1.3	1.22
Sc	ICP80	ppm	0.5	5.3	4.9	1.9	3.7	5.3	2.2	2.8	2.5	6	3.2	4.1
Ti	ICP80	%	0.01	0.09	0.07	0.05	0.13	0.09	0.11	0.13	0.12	0.09	0.16	0.1
V	ICP80	ppm	2	7	4	4	32	7	13	17	15	7	21	5
Cr	ICP80	ppm	1	36	30	31	53	30	53	50	34	69	81	41
Mn	ICP80	ppm	2	287	339	220	366	285	330	380	378	286	408	419
Fe	ICP80	%	0.01	1.19	1.21	0.84	1.43	1.14	1.27	1.49	1.38	1.2	1.76	1.64
Co	ICP80	ppm	1	3	2	2	6	4	4	4	4	4	6	4
Ni	ICP80	ppm	1	4	5	2	11	3	6	3	5	4	7	4
Cu	ICP80	ppm	0.5	7.1	4.3	2.3	36.3	8.4	3.1	3.8	2.2	12	3.4	3.7
Zn	ICP80	ppm	0.5	49.1	73.2	31.5	38.9	52.7	37	38.6	40.4	53.4	46.7	66.5
As	ICP80	ppm	3	<3	<3	<3	<3	<3	10	21	<3	<3	6	<3
Sr	ICP80	ppm	0.5	60.7	57	98	118	54.7	83.3	107	92.4	65.9	134	177

Table 2. Continued

Element	XRAL Method Code	Unit	Detection limit	PSO[b]	EP1[c]	EB1 G[d]	EB1 B[e]	Jyun[f]	Tok[g]	Gan1[h]	Gan2[h]	Hos1[i]	Hos2[i]	Hos3[i]
Y	ICP80	ppm	0.5	24.3	31.5	7.7	7.9	12.3	16.7	18.4	16.1	17.4	17.4	18.1
Zr	ICP80	ppm	0.5	38.3	28.4	23.8	27.4	36	28.6	24.6	30.5	28.7	23.8	12.3
Mo	ICP80	ppm	1	<1	<1	2	2	2	<1	2	1	2	1	3
Ag	ICP80	ppm	0.2	<0.2	<0.2	0.3	0.2	0.5	0.3	<0.2	<0.2	0.2	0.3	<0.2
Cd	ICP80	ppm	1	<1	<1	<1	<1	<1	<1	<1	<1	<1	<1	<1
Sn	ICP80	ppm	10	<10	<10	<10	<10	<10	<10	<10	<10	<10	<10	<10
Sb	ICP80	ppm	5	<5	<5	6	<5	<5	<5	<5	<5	<5	<5	7
Ba	ICP80	ppm	1	400	309	666	298	298	356	433	431	380	545	431
La	ICP80	ppm	0.5	24.4	14	19.4	9.2	19.3	14.3	19.3	17.8	23.3	20.9	16.7
W	ICP80	ppm	10	<10	<10	<10	<10	<10	<10	<10	<10	<10	<10	<10
Pb	ICP80	ppm	2	20	18	23	8	22	17	17	18	22	19	18
Bi	ICP80	ppm	5	<5	<5	<5	<5	<5	<5	<5	<5	<5	<5	<5
Li	ICP80	ppm	1	88	68	32	26	86	51	50	49	87	56	50
B	ES_4	ppm	10	<10	<10	<10	10	<10	<10	<10	<10	<10	<10	<10
Y	MS90	ppm	1	59	50	24	12	58	24	26	24	53	25	29
La	MS90	ppm	0.1	38.7	20.1	23.9	12.6	25.1	16.5	24.9	20.7	27.5	23.9	21
Ce	MS90	ppm	0.1	79.2	44.1	45.8	22.5	55.2	34.4	47.3	36.4	56.7	44.3	43.5
Nd	MS90	ppm	0.1	41.1	25.4	19.7	11.8	31	17.4	20.1	17.5	31.6	18.8	22
Sm	MS90	ppm	0.1	10.2	7.2	4.1	2	8.1	4	4.1	4	8.4	4.2	5.3
Eu	MS90	ppm	0.05	0.46	0.42	0.52	0.38	0.38	0.41	0.39	0.41	0.48	0.59	0.63
Gd	MS90	ppm	0.1	9.9	8.4	4	2.4	9.1	3.7	4.1	4	9.4	4	5.3
Tb	MS90	ppm	0.1	1.6	1.4	0.7	0.4	1.5	0.5	0.7	0.6	1.5	0.6	0.9
Dy	MS90	ppm	0.1	10	9	3.9	2.1	9.9	3.5	4.2	4	8.7	3.5	4.8
Ho	MS90	ppm	0.05	1.89	1.86	0.88	0.43	1.93	0.86	0.82	0.8	1.69	0.76	1.07
Er	MS90	ppm	0.1	5.8	5.3	2.4	1.4	6	2.5	3	2.5	5.6	2.4	3.1
Tm	MS90	ppm	0.1	0.9	0.7	0.3	0.2	0.8	0.5	0.5	0.4	0.9	0.3	0.4
Yb	MS90	ppm	0.1	5.5	5.4	2.2	1.2	6.3	3.2	3.3	2.9	5.9	2.6	2.8
Lu	MS90	ppm	0.05	0.81	0.67	0.33	0.21	0.87	0.45	0.4	0.4	0.89	0.36	0.35
Th	MS90	ppm	0.1	39	27.7	37.6	5.9	25.4	29.5	19.4	18.4	21.7	15.2	9.4
U	MS90	ppm	0.1	6.1	6.8	4.4	1.4	4.5	4.9	3.8	3.2	4	2.9	2.2
Pr	MS90	ppm	0.1	10.4	6	5.9	3.1	7.6	4.6	5.8	5.1	7.3	5.6	6.1
Cl	CHM113	ppm	50	87	62	64	238	106	161	161	126	81	188	87

[a]LOI: loss of ignition; [b]PSO: Postal Savings Office; [c]EP1: E-building ditch cover granite; [d]EB1 G: E-building facade granite; [e]EB1 B: E-building facade concrete; [f]Jyun: gravestone Jyuonkyoji; [g]Tok: gravestone Tokueiji; [h]Gan1, 2: gravestones Ganjyoji; [i]Hos1, 2, 3: gravestones Hosenji

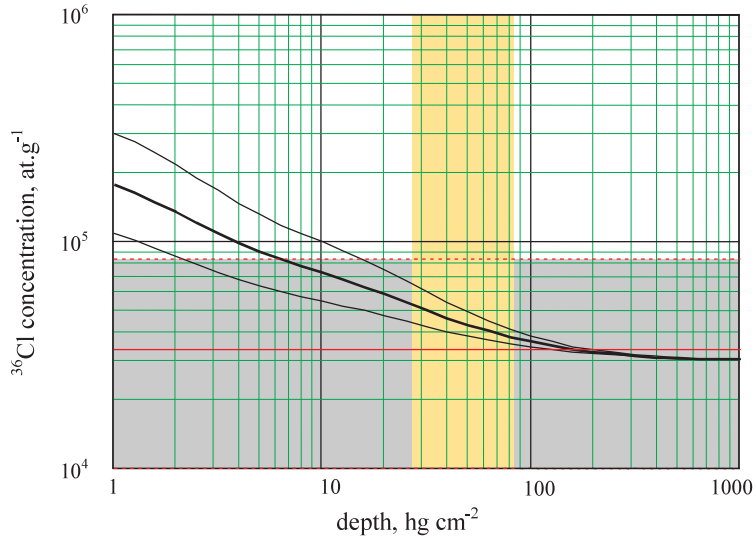

Figure 1. *^{36}Cl atoms/g concentrations calculated for the unexposed Aji granite sample, assuming erosion rates of 50 (upper curve), 100 (middle curve) and 200 μm/a (lower curve). The elemental compositions were taken from Table 1. The grey horizontal band indicates the ^{36}Cl concentration measured in that sample—the point estimate represented by a red solid line, and the experimental uncertainties by red dotted lines that form the boundary of the grey area. The vertical yellow area marks the range of possible depths in the lithosphere from which the sample was supposedly taken; see also Table 3.*

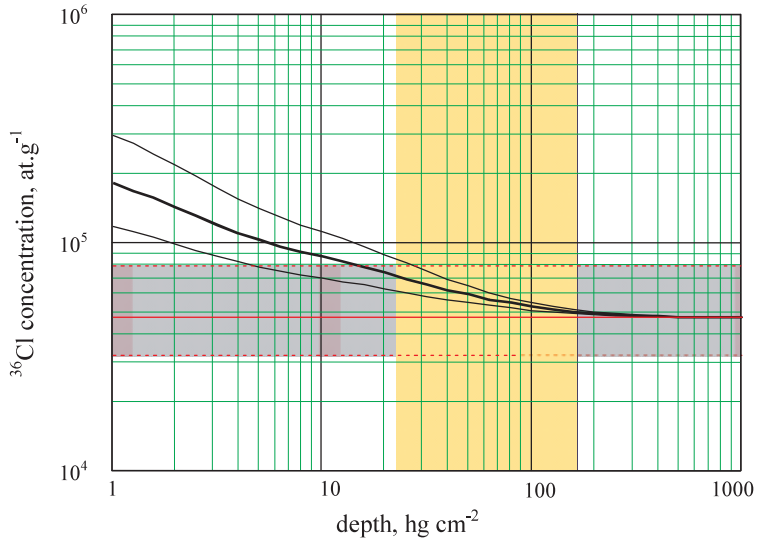

Figure 2. *Same as Figure 1, but for the unexposed Iyo granite sample. The mean of the elemental composition of samples Iyo A and Iyo B (Table 1) was used in the calculations.*

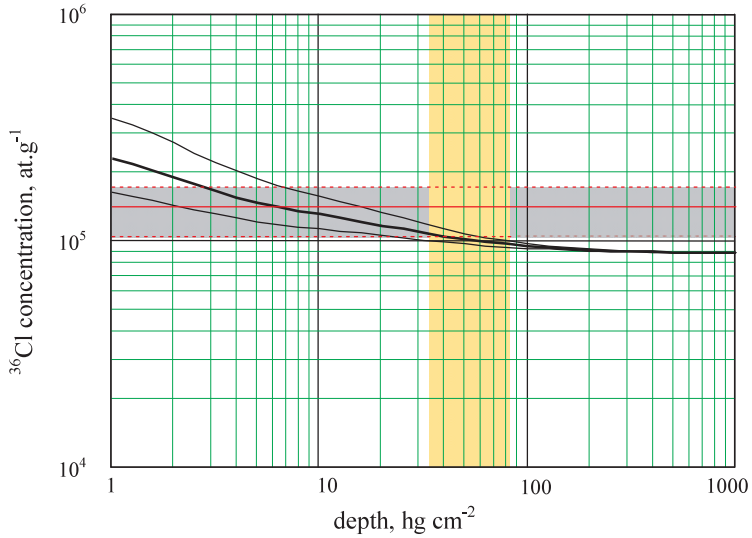

Figure 3. *Same as Figure 1, but for the unexposed Giin granite sample. The mean of the elemental composition of samples Giin A and Giin B (Table 1) was used in the calculations.*

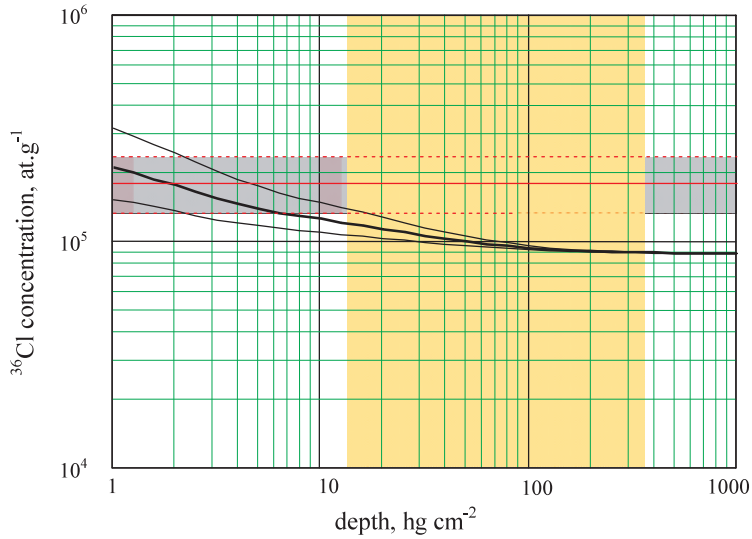

Figure 4. *Same as Figure 1, but for the unexposed Odachi granite sample.*

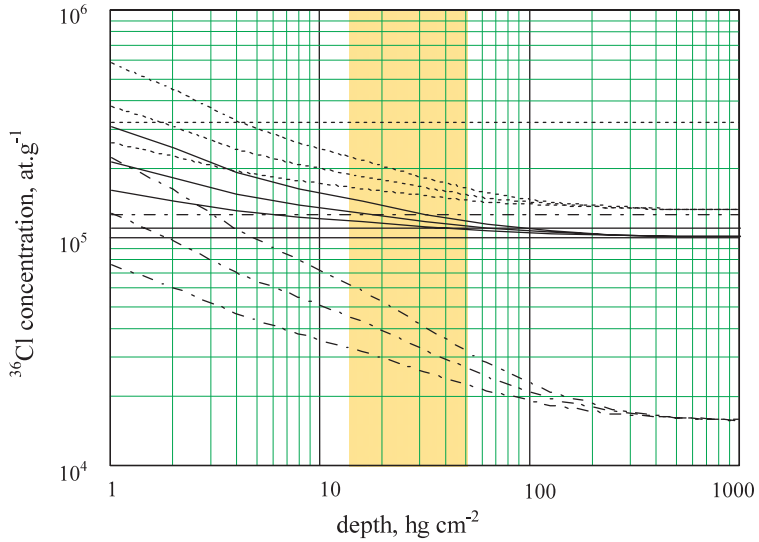

Figure 5. *^{36}Cl atoms/g concentrations calculated for the exposed granite samples of Hosenji 2 (broken line), wall of E-building (solid line) and Saikoji (point broken line). For each sample, erosion rates of 50 (upper curve), 100 (middle curve) and 200 μm/a (lower curve) were used, and the corresponding ratios of ^{36}Cl/Cl =10^{-13} are shown by horizontal lines of the same type. The vertical yellow area marks the range of possible depths in the lithosphere from which the sample was supposedly taken (5 m - 15 m). The elemental compositions were taken from Table 2.*

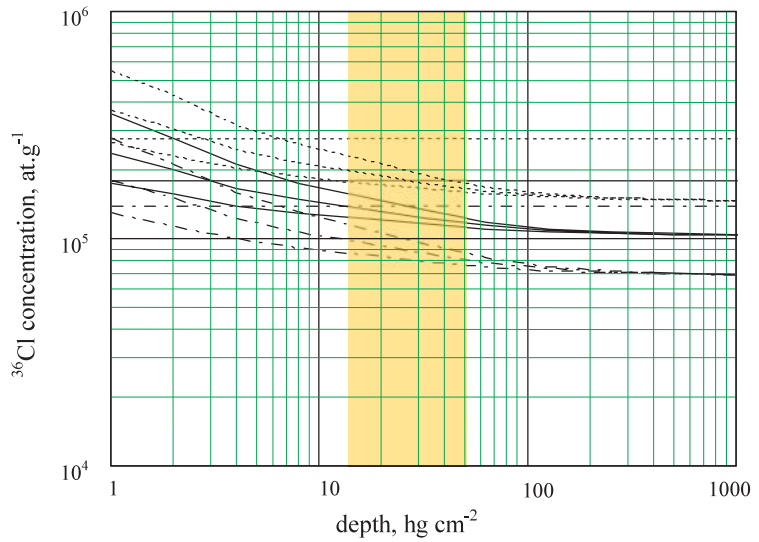

Figure 6. *Same as Figure 5, but for Ganjyoji 1 (dotted line), Jyunkyoji (solid line) and Hosenji 1 (point broken line).*

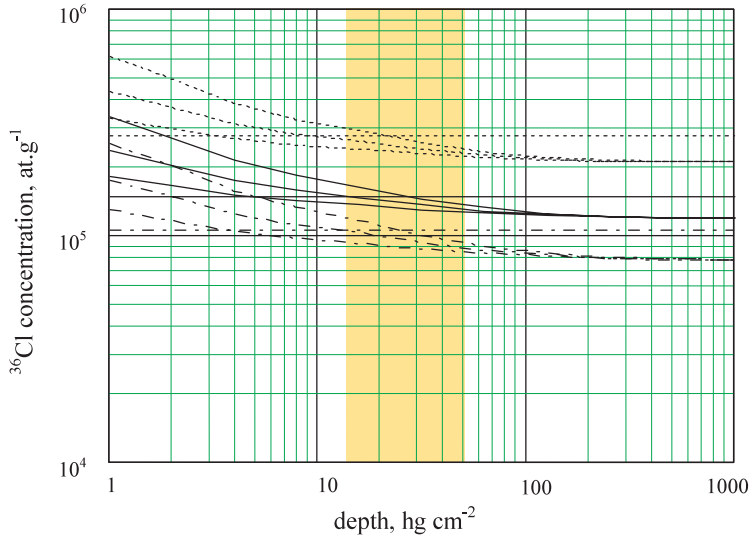

Figure 7. *Same as Figure 5, but for Tokueiji (dotted line), the Postal Saving Office (solid line) and the E-building ditch cover (point broken line).*

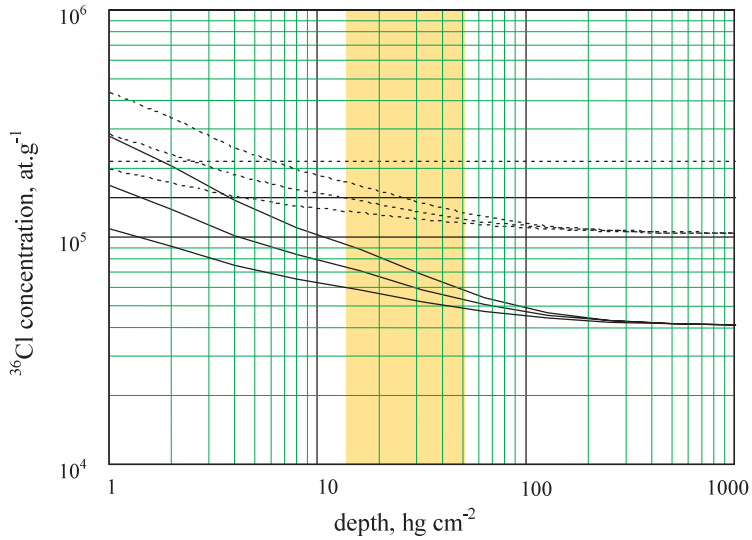

Figure 8. *Same as Figure 5, but for Ganjyoji 2 (dotted line) and Hosenji 3 (solid line).*

In contrast, due to the high U and Th content measured in Giin-type granite, the calculated profile is not that steep, and the exact knowledge of the depth from which the granite was taken is not very critical. At great depths, the calculated ^{36}Cl concentration levels off at about 9×10^4 ^{36}Cl atoms /g, which would correspond, with a stable chlorine content of 100 ppm, to a ^{36}Cl/Cl ratio of about 5×10^{-14} (Figure 3).

Comparison with ^{36}Cl/Cl Ratios Measured by AMS

In Table 3, the experimental results obtained for the investigated granite samples not exposed to A-bomb neutrons are shown in terms of ^{36}Cl/Cl ratios and compared with those calculated on the basis of the elemental composition of the samples given in Table 1, the estimated depths from which the samples were most likely taken, an erosion rate of ε =100 $\mu m/a$, and the methodology described above.

From Figures 1 through 4, it can be deduced that the ^{36}Cl concentrations calculated for the unexposed granite samples are in reasonable agreement with the measured concentrations, for an erosion rate of 100 μm/a, which has been deduced from ^{40}Ar. In general, the corresponding calculated ^{36}Cl/Cl ratios including error bars cover a range from 0.2 to 1.6×10^{-13} and average about 0.6×10^{-13}. It turns out that measured ^{36}Cl/Cl ratios are very low for Aji-type and Iyo-type granite, as is also expected from the calculations. Kurahashi-type granite showed somewhat higher ratios of $(0.8 \pm 0.2) \times 10^{-13}$ (Giin) and $1.2\ (+0.4\ -0.3) \times 10^{-13}$ (Odachi), respectively. Though our calculations would also suggest higher ^{36}Cl/Cl ratios for Kurahashi-type granite, compared to those for Aji-type and Iyo-type granite, the measured ^{36}Cl/Cl ratios appear to be somewhat larger than expected. This seems to hint that local erosion rates on Kurahashi Island were somewhat lower than the 100 $\mu m/a$ assumed in the calculations. In principle, the depth estimate introduces another uncertainty, in particular for the exposed granite sample where it is difficult to obtain reliable information. This uncertainty could be removed by measuring, in these samples, other long-lived radionuclides such as ^{10}Be and ^{26}Al for which production is dominated by cosmic-ray induced reactions, rather than by neutrons originating from the Hiroshima bomb.

From Figures 5 through 8, it can be inferred that ^{36}Cl/Cl ratios deduced here for the other exposed granite samples, using an estimated depth range of 10 ± 5 m and an erosion rate of ε = 100 $\mu m/a$, are generally in the range of 10^{-13}. For example, the granite samples from the E-building are supposed to be Giin-type granite from Kurahashi Island. In those samples *exposed* to A-bomb neutrons, ^{36}Cl/Cl ratios close to 10^{-13} were measured (Chapter 8, Part E), which is close to the values measured here for the *unexposed* Giin sample, and also to the ratios calculated for natural *in situ* production with the methodology described above. Therefore, it is concluded that a significant portion of ^{36}Cl measured in line-of-sight granite samples from the E-building (Chapter 8, Part E) is due to cosmic radiation or to neutrons originating from U and Th decays. For this reason, the assessment of ^{36}Cl induced by A-bomb neutrons in mineral samples from Hiroshima becomes increasingly difficult at ground ranges beyond about 1,200 m.

Concrete samples are composite samples, and no information on the origin of the separate components is available. Therefore, calculations of the natural *in situ* production of ^{36}Cl were not performed for concrete. However, if individual components of the concrete such as the pebbles are separated and measured, calculations for those components could be performed under the assumption that the samples originated from the surface of the Earth.

If the ^{36}Cl/Cl ratio calculated with DS02 for the seven concrete samples of the E-building

(0.55×10^{-13}) is subtracted from the mean value measured for those samples [$(0.74 \pm 0.08) \times 10^{-13}$; Chapter 8, Part E] the resulting ^{36}Cl/Cl ratio of $(0.2 \pm 0.1) \times 10^{-13}$ can be interpreted as a rough estimate for the natural *in situ* production of ^{36}Cl in these samples. For this estimate, any uncertainty that might be associated with the DS02 calculation was not taken into account.

Conclusions

In the present paper, a method was developed to calculate the contribution of natural *in situ* production of ^{36}Cl in mineral samples to the ^{36}Cl signal induced by the neutrons from the Hiroshima bomb. Parameters used in the calculations include local erosion rates, lithospheric depth, and elemental composition for each investigated sample. It has been shown that the calculations agree within their uncertainties with ^{36}Cl values measured by means of accelerator mass spectrometry, in granite samples from quarries with known locations. Both calculations and measurements suggest typical ^{36}Cl/Cl ratios of about 10^{-13} in mineral samples.

For mineral samples exposed to neutrons originating from the Hiroshima bomb, ^{36}Cl/Cl ratios of about 10^{-13} are expected at a ground range of about 1,200 m. Thus, the calculation of the *in situ* production of ^{36}Cl is indispensable in determining the ^{36}Cl background levels in mineral samples exposed to neutrons from the Hiroshima bomb at ground ranges beyond about 1,000 m. For those samples, a comparison of calculated natural *in situ* production of ^{36}Cl and measured ^{36}Cl levels is given in Chapter 8 Part E.

For short-lived radionuclides such as ^{60}Co and ^{152}Eu, natural *in situ* production does not contribute significantly to the production by neutrons originating from the A-bombs, even at large distances from the hypocenter in Hiroshima, because of their shorter half-lives.

Table 3. Measured ^{36}Cl/Cl ratios for the four granite samples from the Aji, Giin, Iyo and Odachi quarries that were not exposed to A-bomb neutrons

Type of granite	Location of quarry	Distance to Hiroshima [km]	Depth from the surface [m]	^{36}Cl/Cl [10^{-13}] (measured)	^{36}Cl/Cl [10^{-13}] (calculated)[a]
Giin	Kurahashi-cho, Hiroshima Pref.	33	10 – 30	0.8 ± 0.2	0.59 – 0.66
Odachi	Kurahashi-cho, Hiroshima Pref.	33	7 – 100	$1.2\ ^{+0.4}_{-0.3}$	0.61 – 0.78
Aji	Aji-cho, Kagawa Pref.	155	10 – 30	$0.2\ ^{+0.3}_{-0.2}$	0.24 – 0.31
Iyo	Miyakubo-cho, Ehime Pref.	60	5 – 60	0.3 ± 0.1	0.30 – 0.50

[a]Calculations were performed on the basis of the elemental composition of the samples given in Table 1, the estimated depths from which the samples were supposedly taken, an erosion rate of $\varepsilon = 100\ \mu m/a$, and the methodology described above.

Acknowledgments

This work was partially supported by BMBF (German Federal Ministry of Education and Research), BMU (German Federal Ministry of Environment, Nature Conservation and Nuclear Safety, and DFG (German Research Council). The authors would like to thank F. Kubo and H. Reithmeier for their help during the AMS beam times.

References

Dockhorn, B.; Neumaier, S.; Hartmann F. J.; Petitjean, C.; Faestermann, H.; Korschinek, G.; Morinaga, H.; Nolte, E. "Determination of erosion rates with cosmic ray produced ^{36}Cl." *Z. Phys. A—Hadrons and Nuclei* 341: 117-119; 1991.

Egidy von, T.; Hartmann, F. J. "Average muonic Coulomb capture probabilities for 65 elements." *Phys. Rev.* A26: 2355-2360; 1982.

Feige, Y.; Oltman, B. G.; Kastner, J. "Production Rates of Neutrons in Soils Due to Natural radioactivity." *J. Geophys. Res.* 73: 3135-3142; 1968.

Fujiwara, O.; Sanga, T.; Ohmori, H. "Regional distribution of erosion rates over the Japanese Islands." Japan Nuclear Cycle Development Institute, *JNC Tech. Rev.* No. 5: 85-93; 1999. (in Japanese)

Haberstock, G.: Heinzl, J.: Korschinek, G.; Morinaga, H.; Nolte, E.; Ratzinger, U.; Kato, K.; Wolf, M. "Accelerator mass spectrometry with fully stripped ^{36}Cl ions." *Radiocarbon* 28: 204-210; 1986.

Hagner, T.; von Hentig, R.; Heisinger, B.; Oberauer, L.; Schonert, S.; von Feilitzsch, F.; Nolte, E. "Muon-induced production of radioactive isotopes in scintillation detectors." *Astroparticle Phys*, 14: 33-47; 2000.

Heisinger, B.; Niedermayer, M.; Hartmann, F. J.; Korschinek, G.; Nolte, E.; Morteani, G.; Neumaier, S.; Petitjean, C.; Kubik, P.; Synal, A.; Ivy-Ochs, S. "In situ production of radionuclides at great depths." *Nucl. Inst. Meth.* B123: 341-346; 1997.

Heisinger, B.; Nolte, E. "Cosmogenic in situ production of radionuclides: Exposure ages and erosion rates." *Nucl. Inst. Meth.* B172: 790-795; 2000.

Heisinger, B.; Lal, D.; Jull, A. J. T; Kubik, P.; Ivy-Ochs, S.; Neumaier, S.; Knie, K.; Lazarev, V.; Nolte, E. "Production of selected cosmogenic radionuclides by muons, 1. Fast muons." *Earth Planet. Sci. Lett.* 200: 345-355; 2002a.

Heisinger, B.; Lal, D.; Jull, A. J. T; Kubik, P.; Ivy-Ochs, S.; Knie, K.; Nolte, E. "Production of selected cosmogenic radionuclides by muons. 2. Capture of negative muons." *Earth Planet. Sci. Lett*. 200: 357-369; 2002b.

Kubik, P.; Korschinek, G.; Nolte, E. "Accelerator mass spectrometry with completely stripped ^{36}Cl at the Munich postaccelerator." *Nucl. Inst. Meth.* B1: 51-59; 1983.

Kubik, P.; Korschinek, G.; Nolte, E.; Ratzinger, U.; Ernst, H.; Teichmann, S.; Morinaga, H.; Wild, E.; Hille, P. "Accelerator mass spectrometry of ^{36}Cl in limestone and some paleontological samples using completely stripped ions." *Nucl. Inst. Meth*. B5: 326-330; 1984.

Nakano, K. Kurahashi-Sekizai-Kogyo Co., Ltd., Personal communication with K. Kato, Hiroshima Prefectural College of Health Sciences, Mihara, Japan, 2001.

Oda, M. President of Yamanishi-Sekizai Co., Ltd, and Present Chairman of the Board of Directors for the Ohshima Stone-Maker's Cooperative, Personal communication with K. Kato, Hiroshima Prefectural College of Health Sciences, Mihara, Japan, 2001.

Roesch, W. C.; ed. *US-Japan Joint Reassessment of Atomic Bomb Radiation Dosimetry in Hiroshima and Nagasaki, Final Report.* Hiroshima, Japan: Radiation Effects Research Foundation; 1987.

Rühm, W. "Das Neutronenspektrum von Hiroshima und das Dosimetriesystem DS86," PhD Thesis, Technische Universität München, Munich, Germany, 1993.

Singer, P. "Emission of Particles Following Muon Capture in Intermediate and Heavy Nuclei." In: *Springer Tracts in Modern Physics 71, Nuclear Physics*, pp. 39-87. Berlin-Heidelberg, Germany: Springer; 1974.

Suzuki, T.; Measday, D. F.; Roalsvig, J. P. "Total nuclear capture rates for negative muons." *Phys. Rev.* C35: 2212-2224, 1987.

Tanimura, T. Iwasaki Marble Co., Ltd. , Hiroshima, Personal communication with K. Kato, Hiroshima Prefectural College of Health Sciences, Mihara, Japan, 2001.

Tolstikhin, I., Private communication, 2003.

Yuhara, M.; Kagami, H.; Yuhara, M. "Geochronological study of the Aji granite in the eastern Sanuki district, Ryoke belt, Southwest Japan (Abstract)." In: *The Joint Meeting for Earth and Planetary Science.* Tokyo, Japan, Gb-009; 1999.